DMD Fast Forward. Published on February 23, 2018 as DOI: 10.1124/dmd.117.079855
This article has not been copyedited and formatted. The final version may differ from this version.

BIOSYNTHESIS AND IDENTIFICATION OF METABOLITES OF MARAVIROC AND THEIR USE IN EXPERIMENTS TO DELINEATE THE RELATIVE CONTRIBUTIONS OF CYTOCHROME P4503A4 VS. 3A5

Elaine Tseng, Gwendolyn D. Fate, Gregory S. Walker, Theunis C. Goosen, and R. Scott Obach

Pfizer Inc., Groton, CT, USA

Running Title: Metabolism of Maraviroc by CYP3A4 and CYP3A5

Addresses for Correspondence

Gwendolyn D. Fate
Athena DMPK LLC
29 Willow Lane
East Lyme, CT, 06333
gwenfate@gmail.com

or

R. Scott Obach
Pfizer Inc.
Eastern Point Rd.
Groton, CT, USA, 06340
r.scott.obach@pfizer.com

Number of Words in:
Abstract: 211
Introduction 352
Discussion 925
Number of References: 21
Number of Tables: 2
Number of Figures: 8

List of Abbreviations: NADPH: nicotinamide adenine dinucleotide phosphate, reduced form; EM: extensive metabolizer; HLM: human liver microsomes; MVC: maraviroc; PM: poor metabolizer

DMD Fast Forward. Published on February 23, 2018 as DOI: 10.1124/dmd.117.079855
This article has not been copyedited and formatted. The final version may differ from this version.

Abstract

Maraviroc (MVC) is an CCR5 co-receptor antagonist indicated in combination with other antiretroviral agents for the treatment of CCR5-tropic human immunodefinciency virus-1 (HIV-1) infection. In this study, the metabolism of MVC was investigated in human liver microsomes to delineate the relative roles of CYP3A4 and CYP3A5. MVC is metabolized to five hydroxylated metabolites, all of which were biosynthesized and identified using mass and NMR spectroscopy. The sites of metabolism were the 2- and 3-positions of the 4,4-difluorocyclohexyl moiety and the methyl of the triazole moiety. Absolute configurations were ultimately ascertained by comparsion to authentic standards. The biosynthesized metabolites were utilized for quantitative in vitro experiments in liver microsomes using cyp3cide, a selective inactivator of CYP3A4. (1S,2S)-2-OH-MVC was the main metabolite representing approximately half of total metabolism, and CYP3A5 contributed approximately 40% to that pathway in microsomes from CYP3A5 *1/*1 donors. The other four metabolites were almost exclusively metabolized by CYP3A4. (1S,2S)-2-hydroxylation also correlated to T-5 N-oxidation, a CYP3A5 specific activity. These data are consistent with clinical pharmacokinetic data wherein CYP3A5 extensive metabolizer subjects showed a modestly lower exposure to MVC.

DMD Fast Forward. Published on February 23, 2018 as DOI: 10.1124/dmd.117.079855
This article has not been copyedited and formatted. The final version may differ from this version.

Introduction

Maraviroc (MVC) is a human chemokine (C-C motif) receptor 5 (CCR5) antagonist indicated in combination with other antiretroviral agents for the treatment of CCR5-tropic human immunodefinciency virus-1 (HIV-1) infection (Dorr et.al. 2005). HIV-1 strains use CCR5 as a coreceptor during the transmission stage and in the early stages of HIV disease (Michael et al., 1997; Philpott, 2003). Blocking the CCR5 receptor prevents entry of HIV into host cells and is shown to reduce viral load to undetectable levels in both treatment naïve and treatment experienced populations and is sustained out to five years of follow up. MVC is rapidly absorbed and extensively metabolized, although unchanged MVC is the major circulating component in plasma and is the major excreted component after oral dosing. Previous in vitro experiments showed that MVC undergoes oxidative metabolism mediated by CYP3A4 (Hyland et al., 2008). Renal clearance contributes 23% of total clearance and the absolute bioavailability of 100 mg oral MVC dose is 23% (estimated at 33% for 300 mg dose). (Abel et al., 2008, 2009; Vourvahis, et al., 2013). A recent publication by Lu et al. (2014) described the effects of the CYP3A5 genotype on MVC plasma concentrations. Those results suggested that CYP3A5 may play a prominent role in the metabolism of MVC in subjects with functional CYP3A5 alleles. This was in line with data in human liver microsomes (HLMs) showing that the estimated CYP3A5 contribution to MVC metabolism in HLMs from wild-type CYP3A5 *1/*1 donors (extensive metabolizers; EMs) was 32% compared with only 2% in HLMs from CYP3A5 *3/*3 donors (poor metabolizers; PM) (Tseng et al., 2014).

In this paper we describe the biosynthesis and identification of four metabolites that are hydroxylated on the difluoro cyclohexyl moiety, out of eight possible regio- and stereoisomers, along with a fifth wherein hydroxylation is on the methyltriazole moiety. The contribution of

CYP3A5 to their formation was quantitatively delineated through the use of pooled human liver microsomes from CYP3A5 *1/*1 genotype donors, the CYP3A4 selective inactivator cyp3cide (Walsky, et al., 2012), the CYP3A5 selective reaction T-5 N-oxidation (Li, et al., 2014), and recombinant heterologously expressed CYP3A4 and CYP3A5.

DMD Fast Forward. Published on February 23, 2018 as DOI: 10.1124/dmd.117.079855
This article has not been copyedited and formatted. The final version may differ from this version.

Materials and Methods

Materials. MVC, d_5-MVC, T-5 (methyl 2-(4-aminophenyl)-1-oxo-7-(pyridin-2-ylmethoxy)-4-(3,4,5-trimethoxyphenyl)-1,2-dihydroisoquinoline-3-carboxylate), T-5 N-oxide, and cyp3cide were prepared at Pfizer (Groton, CT). OH-MVC and deuterated OH-MVC isomers were biosynthesized as described below; chemical synthesis of all eight 2- and 3-OH-MVC isomers are described in the Supplemental Information. Ketoconazole, terfenadine, and NADPH was obtained from Sigma-Aldrich (St. Louis, MO). A 50-donor pool of human liver microsome (HLM-102; equal females and males) was prepared under contract by BD Gentest (Woburn, MA). Single genotyped human liver microsomes (HLM) used in this study are similar to those from Walsky et al. (2012). [*CYP3A5 *1/*1*: HH47, BD HH785, BD HH867, BD HH860, HH86, HH103, HH104, and HH107; *CYP3A5 *1/*3*: HH1, HH2, HH8, HH9, HH80, HH89, HH90, HH91, HH92, HH108, HH117, HH48, and HH100; *CYP3A5 *3/*3*: BDHH189, HH25, HH116, HH118, HH74, HH75, HH98] were obtained from BD Biosciences (San Jose, CA). The BD designation in front of some microsomal donor samples indicates the sample has been genotyped and immunoquantified for CYP3A4 and CYP3A5 by BD Biosciences; otherwise, the donor characterizations were conducted by Pfizer, Inc. Pooled lots of HLM CYP3A5 *1/*1 (from 5 donors; 2 females, 3 males) and HLM CYP3A5 *3/*3 (from 6 donors; 1 female, five males) were prepared by pooling equal volumes of some of the individual lots above such that the resulting enzymatic activity (measured by 6β-OH testosterone formation) is similar between the two lots. Recombinant heterologously expressed CYP3A4 and CYP3A5 were prepared under contract by Panvera Corp. (Madison, WI). All other chemicals and reagents were from standard suppliers.

DMD Fast Forward. Published on February 23, 2018 as DOI: 10.1124/dmd.117.079855
This article has not been copyedited and formatted. The final version may differ from this version.

Metabolism of Maraviroc by Recombinant CYP3A4 and 3A5. MVC (10 μM) was incubated with recombinant human CYP3A4 or CYP3A5 both at 100 pmol/mL, in 100 mM potassium phosphate buffer (pH 7.4) with $MgCl_2$ (3.3 mM) and NADPH (1.3 mM) at 37°C in a shaking water bath for 1 hr. The incubation was commenced with the addition of NADPH and terminated with the addition of acetonitrile (5 mL). The mixture was spun in a centrifuge at 1700g for 5 min, the supernatant was transferred to a vacuum centrifuge, and the liquid removed in vacuo. The residue was reconstituted in 0.2 mL water containing methanol (5%) and formic acid (1%) and analyzed by UHPLC-UV-MS.

Separation of OH-MVC Isomers by UHPLC-UV-MS. Samples (10 μL) were injected onto a Thermo Orbitrap Elite mass spectrometer with an Accela UHPLC-UV system. Separation was effected on an Acquity HSS T3 column (2.1 x 100 mm 1.8μm; Waters) maintained at 45°C. The mobile phase was composed of 0.1% formic acid in water (A) and methanol (B) at a flow rate of 0.4 mL/min. The mobile phase gradient was as follows: 0-15 min linear gradient from 15% B to 25% B, linear gradient to 90% B at 19 min, held at 90% B for 1 min, and re-equilibration to initial conditions for 1 min. The UV detector was monitored from 200 to 400 nm. The mass spectrometer was operated in the positive mode, with source conditions and potentials adjusted to optimize the signal and fragmentation of MVC, and a resolution setting of 30000.

Biosynthesis of OH-MVC Metabolites. MVC (20 μM) was incubated with recombinant CYP3A5 (5.04 nmoles) in 43 mL KH_2PO_4 (0.1 M) containing $MgCl_2$ (3.3 mM) and NADPH (1.3 mM). The incubation was carried out at 37°C for 1.75 hr in a shaking water bath. The reaction was terminated with the addition of acetonitrile (50 mL), the mixture was centrifuged at 1700g for 5 min, and the supernatant was reduced *in vacuo* to ~10 mL. To the remaining material was added formic acid (0.5 mL), acetonitrile (0.5 mL), and water to a total volume of 50

mL, and the mixture was spun in a centrifuge for 30 min at 40000g. The resulting supernatant was applied through a Jasco pump onto a Polaris C18 column (4.6 x 250 mm; 5µm) at a flow rate of 0.8 mL/min. After the entire volume was applied, the column was moved to a Thermo-Finnigan Surveyor HPLC-UV in line with an LTQ MS, and a mobile phase gradient was applied to elute the metabolites. The mobile phase consisted of 0.1% formic acid in water (A) and acetonitrile (B) at a flow rate of 0.8 mL/min. The composition began at 1% B followed by an immediate increase to 5% B held for 4 min, followed by a linear gradient to 40% B at 100 min, an immediate increase to 95% B to wash the column for 10 min, and reequilibration to initial conditions for 10 min. The eluent passed through the UV detector and was then split approximately 10:1 between a fraction collector and the mass spectrometer. Fractions were collected every 20 sec. Fractions potentially containing metabolites of interest were injected on the UHPLC-MS system described above to test for identity and apparent purity. Fractions were combined as appropriate, and the solvent was removed *in vacuo*.

NMR Sample Analysis. Isolated samples and standards were reconstituted in 0.04 mL of methanol-d_4 "100%" (Cambridge Isotope Laboratories, Andover, MA) and placed in a 1.7 mm NMR tube under a dry argon atmosphere. The ^{1}H and ^{13}C spectra were referenced using residual methanol-d_3 (^{1}H δ=3.35 ppm relative to TMS, δ=0.00, ^{13}C δ=49.5 ppm relative to TMS, δ=0.00). NMR spectra were recorded on a Bruker Avance 600 MHz (Bruker BioSpin Corporation, Billerica, MA) controlled by Topspin V3.2 and equipped with a 1.7 mm TCI Cryo probe. 1D spectra were recorded using an approximate sweep width of 8400 Hz and a total recycle time of approximately 7 s. The resulting time-averaged free induction decays were transformed using an exponential line broadening of 1.0 Hz to enhance signal to noise. The 2D data were recorded using the standard pulse sequences provided by Bruker. At minimum a 1K x 128 data matrix

DMD Fast Forward. Published on February 23, 2018 as DOI: 10.1124/dmd.117.079855
This article has not been copyedited and formatted. The final version may differ from this version.

was acquired using a minimum of 2 scans and 16 dummy scans with a spectral width of 10000 Hz in the f2 dimension. The 2D data sets were zero-filled to at least 1k data point. Post-acquisition data processing was performed with either Topspin V3.2 or MestReNova Mnova 9.1. Quantitation of NMR isolates was performed by external calibration against the ^{1}H NMR spectrum of either a 1 mM maleic acid or a 5 mM benzoic acid standard using the ERETIC2 function within Topspin V3.2.

Metabolism of 2- and 3-OH-MVC Diastereomers to 2,3-DiOH-MVC by Cytochrome P4503A4. OH-MVC isomers (10 μM) were each individually incubated with recombinant CYP3A4 (100 pmol/mL) in 0.5 mL potassium phosphate buffer (100 mM, pH 7.4) containing $MgCl_2$ (3.3 mM) and NADPH (1.3 mM) at 37^{o}C for 1 hr. Incubations were terminated by addition of acetonitrile (2.5 mL) and spun in a centrifuge at 1700g for 5 min. The liquid was removed by vacuum centrifugation in a Genevac and the residue was reconstituted in water containing formic acid (1%) and methanol (5%). The samples (5 μL) were injected onto a Thermo Orbitrap Elite mass spectrometer with an Accela UHPLC-UV system. Separation was effected on an Acquity HSS T3 column was a (2.1 x 100 mm 1.8μm) and two different mobile phase gradients were used. (Two conditions were used to better ensure that dihydroxy MVC metabolites were indeed the same from incubations of different starting materials.) One mobile phase was 0.1% formic acid in water (A) and methanol (B), at a temperature of 45^{o}C. The flow rate was 0.4 mL/min. The mobile phase gradient was as follows: 0-15 min linear gradient from 5% B to 25% B, linear gradient to 90% B at 19 min, held at 90% B for 1 min, and re-equilibration to initial conditions for 1 min. The UV detector was monitored from 200 to 400 nm. The second gradient was comprised of mobile phase A of 10 mM ammonium acetate and mobile phase B was methanol. The gradient started at 30% B and increased linearly to 60% B at

15 min, raised to 90% B at 19 min, held for 1 min, then re-equilibrated for 1 min at the initial conditions. The mass spectrometer was operated in the positive mode, and *m/z* 546 (corresponding to the protonated molecular ion of diOH-MVC) and its fragment ions were monitored.

Substrate Saturation Incubation in Human Liver Microsomes and Human Recombinant CYP3A4 and CYP3A5. MVC (1-200 μM) was incubated in 100 mM potassium phosphate buffer (pH 7.4), 3.3 mM $MgCl_2$, and 0.05 mg/mL microsomal protein (HLM-102, HLM CYP3A5*1/*1, and HLM CYP3A5 *3/*3) or 10 pmol/mL recombinant P450 enzymes (rhCYP3A4 and rhCYP3A5). Incubations were conducted in a 37°C heat block for 15 min. (These incubation conditions were selected after initial exploration of protein/enzyme concentrations and incubation times that provided linear reaction velocities.) Reactions were terminated by transferring 50 μL aliquots of the incubation mixture to 100 μL of 50/50 acetonitrile/methanol containing internal standard (mixture of d_5-OH-MVC metabolites), followed by vortex mixing. Samples were centrifuged (1439 g) for 10 minutes and 120 μL of supernatant was transferred to clean 96-well plates. The supernatants were dried down under N_2 and reconstituted in 100 μL 20/80 methanol/0.1% formic acid in water. Samples were assayed using LC-MS/MS. Incubations for enzyme kinetic determination was conducted with NADPH, in triplicate.

Selective Inhibition of CYP3A4 and CYP3A5 Activity in Human Liver Microsomes. MVC (8 μM) was incubated with HLM-102, HLM CYP3A5*1/*1, or HLM CYP3A5 *3/*3 in the presence of selective chemical inhibitors ketoconazole (1μM; for CYP3A) and CYP3cide (1μM; for CYP3A4), for the determination of CYP3A4 and CYP3A5 isoform contribution. General

incubation conditions (protein concentration and incubation time) and sample preparation were as described for substrate saturation experiments (*vide supra*).

For incubations with ketoconazole, a mixture containing microsomes, inhibitors, and NADPH or buffer (-NADPH control) was warmed for 5 min prior to initiating the reactions by the addition of substrate. Incubations containing CYP3cide were preincubated with microsomes, inactivator, and NADPH or buffer (-NADPH control) for 10 minutes to achieve complete inactivation of CYP3A4 prior to the addition of MVC to initiate the reactions. Chemical inhibition experiments were conducted in triplicate.

LC-MS/MS Method. Supernatants from the terminated incubation mixtures were analyzed using a liquid chromatography mass spectrometry system (LC-MS/MS) consisting of an API6500 mass spectrometer (AB Sciex, Framingham, MA) equipped with an electrospray source, Agilent 1290 Binary UPLC system (Agilent Technologies, Santa Clara, CA) and a Leap CTC HTS PAL autosampler. Chromatography was carried out on a Waters Acquity UPLC HSS T3 column (2.1 x 100 mm; 1.8µ particle size) with a mobile phase comprised of water (A) and methanol (B) containing 0.1% formic acid at a flow rate of 0.4 mL/min. Samples (0.01 mL) were injected and the mobile phase composition was maintained at 20% B for 6.5 min followed by a linear gradient to 35% B over the next 6.5 min, and followed by an increase to 90% B over 0.5 min. It was held at 90% B for another 0.5 min before returning to initial conditions and re-equilibrating to initial conditions for 2 min. Optimized transitions and parameters of MVC, metabolites, and stable label internal standards used for mass spectrometric detection on the AB Sciex Triple Quad 6500 are listed in Supplemental Table S1. Integration and quantitation of metabolites and IS molecule peak areas were performed using Analyst v1.6.2 (AB Sciex, Framingham, MA) and to derive the analyte to IS peak area ratios. Standard curves for the

quantitation of metabolite concentration were prepared from plots of area ratio vs concentration and analyzed using a linear regression with either 1/x or $1/x^2$ weighting.

Correlation Analysis with T5. MVC (8 μM) and T5 (5 μM) were incubated in HLMs from individual donors in triplicate. For MVC, general incubation conditions (protein concentration and incubation time) and sample preparation were as described for substrate saturation experiments. For T5, experimental and analysis conditions were similar to that described by Li, et al. (2014). In general, final incubation mixtures contained 100 mM potassium phosphate buffer (pH 7.4), 3.3 mM $MgCl_2$, and 0.1 mg/mL microsomal protein. Incubations were conducted in a 37°C heat block. Reactions were terminated after 20 min by transferring 50 μL aliquots of the incubation mixture to 100 μL of acetonitrile containing internal standard (terfenadine; 2 ng/mL), followed by vortex mixing. Samples were centrifuged (1439 g) for 10 min and 120 μL of supernatant was transferred to clean 96-well plates. Supernatants from the terminated incubation mixtures were analyzed using the aforementioned liquid chromatography mass spectrometry system. Chromatography was carried out on a Waters Acquity UPLC HSS T3 column (2.1 x 50 mm; 1.8μ particle size) with a mobile phase comprised of water (A) and acetonitrile (B) containing 0.1% formic acid at a flow rate of 0.4 mL/min. Samples (0.01 mL) were injected and the mobile phase composition was maintained at 5% B for 0.5 min followed by a linear gradient to 95% B over 2 min and held at 95% B for another 0.5 min before returning to initial conditions and reequilibrating to initial conditions for 1 min. T5 N-oxide and terfenadine were monitored using mass transitions of *m/z* 584.2-476.2 and *m/z* 472.1 -436.1, respectively.

Results

Profile of OH-MVC Metabolites Generated by Cytochrome P450 3A4 and 3A5. MVC was incubated with recombinant human P450 3A4 and 3A5 and the incubation extracts were analyzed by HPLC-MS. The extracted ion chromatograms for hydroxylated MVC are shown in Figure 1. Five metabolites were resolved, observed eluting between 9 and 18 min. The first four are 2- and 3-hydroxylations on the difluorocyclohexyl moiety and the fifth one is the hydroxyl on the triazole portion (see below). All five were generated by both enzymes, however the intensity of the peak eluting at 9.6 min was greater in the CYP3A5 incubation than the 3A4 incubation. The peaks were shown to coelute with authentic and biosynthesized standards of individual diastereomers of 2- and 3-OH-MVC (Supplemental Information; Figures S1-S5). Also, the other four standards of 2- and 3-OH-MVC isomers were shown to elute at different retention times (Supplemental Figure S6).

Identification of OH-MVC Metabolites. OH-MVC metabolites were biosynthesized using CYP3A4 and CYP3A5, isolated by HPLC, and regiochemical sites of hydroxylation were assigned using high resolution mass spectrometry and NMR spectroscopy. The NMR spectra of metabolites were compared to that of MVC. Exact stereochemical configurations of the hydroxyl isomers on the 4,4-difluorocyclohexyl moiety were ultimately assigned by comparison to authentic standards of all eight possible 2- and 3-hydroxy diastereomers.

2-OH-MVC Isomers. The biosynthesis of OH-MVC metabolites using CYP3A5 and CYP3A4 yielded five products. The ones eluting at ~37-40 min (Fraction 1) and ~51 min (Fraction 4) in the preparative purification (Supplemental Figure S7) were shown to be 2-hydroxy isomers present in CYP3A4 and 3A5 incubation extracts eluting at 9.7 and 17.4 min (Figure 1). The MS^n

data showed protonated molecular ions of *m/z* 530.3285 to 530.3294 (-3 to -1 ppm) and diprotonated molecular ions of *m/z* 265.6677 to 265.6683 (-4 to -1 ppm), with fragment ions of *m/z* 405, 296, 117, and 106 which are diagnostic of the site of hydroxylation as being on the 4,4-difluorocyclohexyl moiety (Supplemental Figures S8 and S9). However, distinction between the 2- and 3-positions required the application of NMR spectroscopy.

In fractions 1 and 4 there is a new resonance in the ^{1}H spectrum of each isolate integrating to a single hydrogen at δ 3.94 (td, J = 10.9, 4.7 Hz) not observed in the ^{1}H spectrum of MVC, Figure 2A. Multiplicity edited ^{1}H – ^{13}C HSQC data correlate these resonances to a carbon resonance with a chemical shift of 67.6 ppm (Supplemental Figures S16 and S19). This is consistent with the oxidation of one of the methylenes of the difluorocyclohexane. Initial NMR characterization of isolates from clinical samples assigned these resonances as the ***H***COH methine of the trans 2-hydroxy MVC isomer. When spectra from fractions 1 and 4 are compared with similarly acquired spectra from a synthetic standard of the 2-hydroxy MVC trans isomers (fraction 1 = 1S, 2S and fraction 4 = 1R, 2R) there are no appreciable differences in the ^{1}H/^{13}C chemical shifts, coupling patterns or coupling constants of these resonances (Supplemental Figures S16 and S19). Therefore the structure of the fractions 1 and 4 are assigned as 2-OH-MVC trans isomers. These structures are further supported by the HPLC coelution of the two biosynthesized standards with the authentic 1S, 2S and 1R, 2R diastereomers and not the 1R, 2S or 1S, 2R diastereomers (Supplemental Figures S1, S2, and S6). Finally, in a previous report (Abel, et al., 2008), these metabolites were ambiguously designated as H7, H8, H10, and/or H11. The present data identifies (1S,2S)-2-OHMVC as H8 and (1R,2R)-2-OH-MVC as H11 which represented 7 and 5% of total dose in excreta, respectively (Supplemental Table S2).

3-OH-MVC Isomers. In the aforementioned biosynthesis, two other isolated peaks eluting at ~43-45 min (Supplemental Figure S7) were shown to be 3-hydroxy isomers present in CYP3A4 and 3A5 incubation extracts eluting at 11.8 and 12.5 min (Figure 1). As with the 2-hydroxyisomers, MS^n data showed protonated molecular ions of *m/z* 530.3287 to 530.3291 (-3 to -2 ppm) and diprotonated molecular ions of *m/z* 265.6678 to 265.6682 (-3 to -2 ppm), with fragment ions of *m/z* 405, 296, 117, and 106 which are diagnostic of the site of hydroxylation as being on the 4,4-difluorocyclohexyl moiety (Supplemental Figures S10 and S11). NMR spectroscopy was required to delineate the 3-position as the regiochemical site of hydroxylation. As with fractions 1 and 4, there are new resonances in the ^1H spectra of fractions 2 and 3 integrating to a single hydrogen at δ 3.90 (broad singlet, fraction 2) and δ 3.78 (ddt, J = 20.1, 11.2, 4.5 Hz, fraction 3) not observed in the ^1H spectrum of MVC (Figure 2B). Multiplicity edited ^1H – ^{13}C HSQC data correlate these resonances to a carbon resonances with a chemical shifts of δ 67.1(fraction 2) and δ 69.6 (fraction 3), (Supplemental Figures S17 and S18). Again this is consistent with the oxidation of one of the methylenes of the difluorocyclohexane. When spectra from fractions 2 and 3 are compared with similarly acquired spectra from synthetic standards of the 3-hydroxy MVC isomers there are no appreciable differences in the $^1H/^{13}C$ chemical shifts, coupling patterns or coupling constants of these resonances (Figure 2B). Therefore the structure of the fractions 2 and 3 are assigned as 3-OH-MVC isomers. Unlike the 2-OH-MVC diastereomers, the chemical synthesis of the 3-hydroxy isomers yielded two sets of stereoisomers (cis and trans) but absolute configurations were not known. Absolute stereochemistry of the 3-OH-MVC metabolites was elucidated using a 'cross-metabolism' approach (*vide infra*).

HydroxymethylMVC. The fifth hydroxyl metabolite of MVC generated by CYP3A was biosynthesized and eluted at ~63-65 min (Fraction 5; Supplemental Figure S7) and corresponded

DMD Fast Forward. Published on February 23, 2018 as DOI: 10.1124/dmd.117.079855
This article has not been copyedited and formatted. The final version may differ from this version.

to the metabolite eluting at 17.8 min in CYP3A4 and CYP3A5 incubation extracts (Figure 1 and Supplemental Figure S5). The protonated and diprotonated ions of *m/z* 530.3290 and 265.6680 (-3 to -2 ppm) show addition of a single oxygen. Unlike the other four metabolites above, the fragmentation was different (Supplemental Figure S12). The fragment ion at *m/z* 389 limits the site of hydroxylation to the triazole moiety, since this ion represents no alteration to the rest of the molecule. The ^{1}H spectrum of fraction 5 contains all of the aromatic and aliphatic resonances of MVC except the methyl of the triazole (Figure 3). Additionally, in the ^{1}H-^{13}C multiplicity edited HSQC there is a new methylene cross peak (δ 1H 4.84/ δ 13C 54.1) not observed in MVC (Supplemental Figure S20). These data are consistent with the oxidation of the methyl of the triazole to an alcohol, 4,4-difluoro-N-((S)-3-((1R,3R,5S)-3-(3-(hydroxymethyl)-5-isopropyl-4H-1,2,4-triazol-4-yl)-8-azabicyclo[3.2.1]octan-8-yl)-1-phenylpropyl)cyclohexane-1-carboxamide. This metabolite corresponds to the previously described H13 metabolite from Abel, et al., (2008) which was excreted as 10% of the dose of MVC (Supplemental Table S2).

Elucidation of the Absolute Stereochemical Configuration of the 3-OH-MVC Metabolites. At the time of their synthesis, the specific configurations of the four 3-OH-MVC diastereomers was not known, however the cis- and trans-configurations were known. One diastereomer in each of these preparations matched a CYP3A generated metabolite. Since the absolute configuration of all four 2-OH-MVC isomers was already known, an approach was taken wherein all eight synthetic 2- and 3-OH-MVC isomers were subjected to further metabolism by CYP3A4 with the intent that specific 2,3-diOH-MVC metabolites would be generated from the individual 2- and 3-OH-MVC substrates and would have identical HPLC-MS properties. If this were the case, then using the known configuration at the 1-position of the 2-OH-MVC which

would be unchanged in a 2,3-dihydroxy metabolite, the configuration of the 1 position of the 3-hydroxy metabolite that yields the same 2,3-dihydroxy metabolite can be inferred. Since this will be one of a pair of diastereomers known to be either cis or trans, the 3-position absolute configuration can be concluded (see Figure 4).

The cis 3-hydroxy isomer eluting at 12.4 min (Figure 1) and (1S,2S)-2-OH-MVC yielded the same diOH-MVC metabolite eluting at 8.9 min (Supplemental Figure S13) with a protonated molecular ion at *m/z* 546.3259 (0.9 ppm). The MS^n spectra showed fragment ions of *m/z* 421, 312, 117, and 106, which narrows the site of hydroxylation to the 4,4-difluorocyclohexyl moiety (Supplemental Figure S14). To confirm that this dihydroxy metabolite generated by the 2- and 3-OH-MVC substrates is the same, the sample was analyzed by HPLC using a different mobile phase condition, and the peaks continued to coelute (Supplemental Figure S13). The known configuration of the 2-OH-MVC substrate at the 1-position is S. The cis 3-OH-MVC substrate that yields the same dihydroxy metabolite were either 1S,3S or 1R,3R, but since it yielded the same dihydroxy metabolite as the (1S,2S)-2-OH-MVC isomer, it can be concluded that the CYP3A generated 3-OH-MVC metabolite that elutes at 12.4 min is the 1S,3S isomer (Figure 8). An identical logic and approach was applied to elucidate the absolute stereochemistry of the 3-OH-MVC metabolite eluting at 11.8 min (Figure 1). In this case, this 3-hydroxy metabolite was shown to be the 1S,3R isomer (Figure 8). The 1S,3S and 1S,3R metabolites correspond to those designated as H7 and H10 in the human radiolabel mass balance study which represented 8% and 9% of dose (Abel, et al., 2008; Supplemental Table S2)

Enzyme Kinetics of Maraviroc in Human Liver Microsomes and Recombinant Human CYPs. Enzyme kinetic parameters and intrinsic clearance values, determined from the formation

DMD Fast Forward. Published on February 23, 2018 as DOI: 10.1124/dmd.117.079855
This article has not been copyedited and formatted. The final version may differ from this version.

of the five metabolites of MVC in rCYP3A4, rCYP3A5, HLM-102, HLM CYP3A5 *1/*1, and HLM CYP3A5*3/*3, are listed in Table 1 and substrate saturation data are presented graphically in Figure 5. The results for all metabolites fit to the Michaelis-Menten model. In general, the estimated K_M for each metabolite was comparable to each other within each enzyme system and generally ranged from 7-19 μM. However, the $CL_{int,app}$ provided an initial indication of which recombinant CYP and genotype is preferential to the formation of each MVC metabolite. While all the metabolites are formed by CYP3A4 and CYP3A5 to a certain extent, (1S,2S)-2-OH-MVC is predominately formed by rCYP3A5 and HLM CYP3A5*1/*1 with values for $CL_{int,app}$ of 0.87 μL/min/pmol P450 and 15.6 μL/min/mg, respectively. HydroxymethylMVC is mainly formed by rCYP3A4, HLM-102, and CYP3A5*3/*3 with CLint,app of 0.31 μL/min/pmol P450, 14.0 μL/min/mg and 10.7 μL/min/mg, respectively.

Selective Inhibition of CYP3A4 and CYP3A5. MVC was incubated in the presence and absence of ketoconazole (2 μM) and CYP3cide (1 μM) in human liver microsomes from either a 50-donor pool or pooled CYP3A5 *1/*1 and CYP3A5*3/*3 donors. The impact on the rate of formation of each metabolite was examined in order to estimate the relative contributions of CYP3A4 and CYP3A5. Inhibition data are listed in Supplemental Table S3.

For HLM-102 and CYP3A5*3/*3 pools (CYP3A5 PM), the estimated CYP3A5 contributions were similar across the five metabolites with less than 12% by CYP3A5. In the CYP3A5*1/*1 pool (CYP3A5 EM), the greatest CYP3A5 contribution was observed only for (1S,2S)-2-OH-MVC (42%). Contribution by CYP3A5 was relatively low (<13%) for the other four metabolites.

Correlation Analysis. T-5 oxidation to an N-oxide metabolite by CYP3A5 was first reported by Li, et al. (2014) as a reaction that is highly correlated with the CYP3A5 genotype and CYP3A5 expression levels in human liver microsome and hepatocytes. Formation of the five OH-MVC

metabolites were compared to T-5 N-oxide formation in individual HLM donors genotyped to be CYP3A5 *1/*1, CYP3A5*1/*3, and CYP3A5*3/*3 expressers. A positive correlation with T-5 N-oxide was observed for the (1S,2S)-2-hydroxy metabolite (Pearson r value of the correlation was 0.81, P<0.0001; Figure 7) while the other four metabolites had no correlation (Supplemental Figure S15). This suggests that CYP3A5 genotype has involvement in the metabolic pathway of the (1S,2S)-2-OH-MVC and not the other metabolites.

Summary of CYP3A Enzyme Contribution to Maraviroc Metabolism Assignment.

Incorporating the estimated apparent intrinsic clearance and fraction of CYP3A5 inhibition of each OH-MVC metabolite in HLM, the total fraction of metabolism contributed by CYP3A5 can be estimated in various batches of human liver microsomes. The in vitro apparent intrinsic clearance ($Cl_{int,app}$) values in CYP3A5*1/*1 HLM were calculated as the ratio of V_{max} to K_M where V_{max} and K_M are kinetic parameters determined in Table 1. $CL_{int,app}$ is the intrinsic clearance for metabolite, and $CL_{int,app,all}$ is the sum of in vitro intrinsic clearance values for all metabolites. The fraction of clearance (f_{CL}) by each metabolite is calculated as the apparent intrinsic clearance of each metabolite divided by the total apparent intrinsic clearance for MVC. The fraction of CYP3A5 inhibition was determined from the chemical inhibition study in HLM incorporating ketoconazole and CYP3cide (Supplemental Table S3). The fraction metabolized (f_m) by CY3A5 for each metabolite is calculated as f_{CL} multiplied by the fraction of CYP3A5 inhibition. The total fraction metabolized by CYP3A5 in the *1/*1 genotype is estimated to be 0.25 (Table 2).

Based on the combined results from enzyme kinetics, HLM chemical inhibition, and correlation analysis assays, CYP3A5 was consistently predicted by both HLM and rhCYPs to

DMD Fast Forward. Published on February 23, 2018 as DOI: 10.1124/dmd.117.079855
This article has not been copyedited and formatted. The final version may differ from this version.

contribute the formation of (1S,2S)-2-OH-MVC while the other four hydroxymethylMVC metabolites were predominantly generated by CYP3A4.

Discussion

The application of metabolite biosynthesis using P450 enzymes, followed by NMR spectroscopy to identify regiochemical sites of metabolism and to quantitate the concentration of the material so that it can be used as an analytical standard, is a powerful and facile approach to conducting drug metabolism studies. In this work, we began by biosynthesizing and isolating the five major CYP3A-generated hydroxyl metabolites of MVC. These had previously been identified, but only reported as Markush structures (Abel, et al., 2008). These biosynthesized metabolites were then used as analytical standards to carry out work to quantitatively assess the potential role of CYP3A5 in the metabolism of MVC. They were also used to justify investment in a lengthy and expensive chemical synthesis of all eight possible isomers of 2- and 3-OH-MVC so that the absolute configuration of these metabolites could be ascertained.

Previous in vitro work reported by Lu, et al., (2012) proposed that CYP3A5 has a major role in the metabolism of MVC. However, quantitation of the metabolites done in that work as well as analysis of human plasma samples (Lu, et al., 2014) was based on mass spectral response using the 4-hydroxyphenyl analogue of MVC that was not the actual metabolite. Because 4-hydroxyphenyl MVC is structurally dissimilar to the identified (1S,2S)-2-OH-MVC metabolite in terms of the electronic character of the phenolic versus the aliphatic hydroxyl moieties, it is likely that the estimation of the M1 concentration reported by Lu et. al. would show some bias compared to the actual concentrations present in clinical plasma samples. The claim of a prominent role for CYP3A5 by Lu et.al. (2012) was based primarily on work in recombinant enzymes without the benefit of a relative activity factor or intersystem extrapolation factor for this enzyme that is necessary in order to quantitatively relate rate data from recombinant heterologously expressed enzymes to activities in liver microsomes or in vivo (Chen, et al.,

2011; Proctor, et al., 2004). The lack of a suitable activity factor makes translating the in vitro results to in vivo contribution problematic.

In the present work, we have used the actual metabolite standards in calibration curves required for quantitation by HPLC-MS. We have also employed the CYP3A4 selective inactivator cyp3cide to quantitatively delineate the role of CYP3A4 vs CYP3A5 in pooled liver microsomes from CYP3A5 *1/*1 donors to get a more reliable estimate of the contribution of CYP3A5 to all five of the major in vitro metabolites. From these data, it can be clearly concluded that CYP3A5 has a contributing role in the generation of the (1S,2S)-2-OH-MVC metabolite (which is most likely the "metabolite 1" described by Lu, et al, 2012), but not the other metabolites. By defining the individual metabolic pathways, determining the intrinsic clearance of their formation to gain knowledge of the fraction that each contributes to the whole, and then delineating the role of CYP3A4 vs CYP3A5 to each the metabolites, we have reconstructed the total picture of MVC metabolism to show that CYP3A5 contributes approximately 25% to the metabolism of MVC in CYP3A5 EMs (Figure 8). This is similar to a previous estimate (32%) made by monitoring depletion of MVC in HLM from a CYP3A5 *1/*1 donor (Tseng et.al. 2014).

CYP3A5 is subject to a genetic polymorphism wherein a larger percentage of individuals of African descent express the enzyme (Roy, et al., 2005; Lamba, et al., 2012). Thus, drugs that are shown to be substrates of CYP3A5 have the possibility to show lower exposure in individuals possessing one or two copies of the CYP3A5*1 allele (i.e. IMs and EMs) But the quantitative impact of CYP3A5 must be weighed against the role that other enzymes, especially CYP3A4 have in the overall metabolism, as well as non-metabolic clearance pathways such as the considerable portion of maraviroc excreted unchanged in urine (Abel, et al., 2008). To date, all

drugs that have been shown to be metabolized by CYP3A5 are also metabolized by CYP3A4, therefore quantitatively assessing the role of CYP3A5 in the metabolism of a compound has been challenging up until the introduction of the CYP3A4 selective inactivator cyp3cide (Walsky, et al., 2012), which permits the activities of CYP3A4 and CYP3A5 to be separated in intact in vitro models of drug metabolism (i.e. human liver microsomes or hepatocytes). The results from this work suggest that CYP3A5 would play a minor but measurable role in the metabolic clearance of MVC in CYP3A5 EM individuals. This has been shown in the clinic wherein CYP3A5 EM subjects have been shown to have between 26-41% lower exposure to MVC and a higher (1S,2S)-2-OH-MVC to MVC exposure ratio, consistent with estimates made from the in vitro data (Vourvahis, manuscript in preparation; Lu, et al., 2014). However it is also the observation that these lower exposures are still in excess of exposures associated with near-maximal MVC virologic efficacy, which may explain why there was no observation of decreased efficacy in CYP3A5 EM patients in the phase 3 efficacy trials of MVC (McFadyen 2008, Vourvahis, et al., 2015). Additionally, it should be noted that in clinical practice, many HIV patients receive MVC in the presence of CYP3A-inhibiting protease inhibitors. Such drugs are potent inhibitors of both CYP3A4 and CYP3A5 (Ernest et.al. 2005, Granfors et.al. 2006) and therefore this could potentially diminish the overall role of CYP3A (both 3A4 and 3A5) in the overall metabolism of MVC in patients receiving these drugs.

Overall, these results demonstrate that CYP3A5 can contribute partially to the generation of the (1S,2S)-2-OH-MVC metabolite. The use of biosynthesized metabolites with quantitative NMR spectroscopy served well to enable the subsequent P450 reaction phenotyping experiments needed to quantitatively evaluate the relative roles of CYP3A4 and 3A5 in the metabolism of MVC. Such an approach can be employed to tackle quantitative in vitro drug metabolism

DMD Fast Forward. Published on February 23, 2018 as DOI: 10.1124/dmd.117.079855
This article has not been copyedited and formatted. The final version may differ from this version.

experiments for other compounds, even when synthetic standards of metabolites are difficult or impossible to obtain.

DMD Fast Forward. Published on February 23, 2018 as DOI: 10.1124/dmd.117.079855
This article has not been copyedited and formatted. The final version may differ from this version.

Acknowledgements

The authors thank the following individuals: Olivier Dirat of the Pharmaceutical Research and Development Department at Pfizer, Sandwich, UK for coordination of the synthesis of 2- and 3-OH-MVC standards conducted at Peakdale Molecular, Jan Szeliga of the Pharmaceutical Research and Development Department, Pfizer, Groton, USA for preparative chromatography of the four synthetic 3-OH-MVC isomers, Mark Savage, Torren Peakman, and Angus Nedderman, formerly of Pfizer, Sandwich, UK who conducted excellent early work on maraviroc metabolism that was used as a starting point for these investigations.

Authorship Contributions

Participated in research design: Tseng, Fate, Walker, Goosen, Obach

Conducted experiments: Tseng, Walker, Obach

Performed data analysis: Tseng, Fate, Walker, Obach

Wrote or contributed to the writing of the manuscript: Tseng, Fate, Walker, Goosen, Obach

References

Abel S, Russell D, Whitlock LA, Ridgway CE, Nedderman ANR, and Walker DK. (2008) Br J Clin Pharmacol. 65(Suppl 1): 60-67.

Abel S, Back DJ, Vourvahis M. (2009) Review. Maraviroc: pharmacokinetics and drug interactions. Antiviral Therapy 14:607-618.

Chen Y1, Liu L, Nguyen K, Fretland AJ (2011) Utility of intersystem extrapolation factors in early reaction phenotyping and the quantitative extrapolation of human liver microsomal intrinsic clearance using recombinant cytochromes P450. Drug Metab Dispos. 39: 373-82.

Dorr P, Westby M, Dobbs S, Griffin P, Irvine B, Macartney M, Mori J, Rickett G, Smith-Burchnell C, and Napier C, et al. (2005) Maraviroc (UK-427,857), a potent, orally bioavailable, and selective small-molecule inhibitor of chemokine receptor CCR5 with broad-spectrum anti-human immunodeficiency virus type 1 activity. Antimicrob Agents Chemother 49:4721–4732.

Ernest CS, 2nd, Hall SD, and Jones DR (2005) Mechanism-based inactivation of CYP3A by HIV protease inhibitors. J Pharmacol Exp Ther 312:583–591.

Granfors MT, Wang JS, Kajosaari LI, Laitila J, Neuvonen PJ, and Backman JT (2006) Differ-

ential inhibition of cytochrome P450 3A4, 3A5 and 3A7 by five human immunodeficiency virus (HIV) protease inhibitors in vitro. Basic Clin Pharmacol Toxicol 98:79–85.

Hyland R, Dickins M, Collins C, Jones H, Jones B (2008) Maraviroc: in vitro assessment of drug-drug interaction potential. Br J Clin Pharmacol. 66:498-507.

Lamba J, Hebert JM, Schuetz EG, Klein TE and Altman RB (2012) PharmGKB summary: very important pharmacogene information for CYP3A5. Pharmacogenet Genomics. 22: 555–558.

Li X, Jeso V, Heyward S, Walker GS, Sharma R, Micalizio GC, and Cameron MD (2014) Characterization of T-5 N-Oxide Formation as the First Highly Selective Measure of CYP3A5 Activity. Drug Metab Dispos. 42: 334–342.

Lu Y, Hendrix CW, Bumpus NN (2012) Cytochrome P450 3A5 plays a prominent role in the oxidative metabolism of the anti-human immunodeficiency virus drug maraviroc. Drug Metab Dispos. 40: 2221-30.

Lu Y, Fuchs EJ, Hendrix CW, Bumpus NN. (2014) CYP3A5 genotype impacts maraviroc concentrations in healthy volunteers. Drug Metab Dispos 42: 1796–1802.

McFadyen L, Jacqmin P, Wade JR, and Weatherley B (2008) Maraviroc exposure-efficacy (<50copies/mL) analysis in HIV-1–infected treatment-naive subjects — ITT population (MERIT study), in: 17th International AIDS Conference, Mexico City, Mexico, August 3–8, 2008. Poster TUPE0053.

Michael NL, Chang G, Louie LG, Mascola JR, Dondero D, Birx DL, Sheppard HW. (1997) The role of viral phenotype and CCR-5 gene defects in HIV-1 transmission and disease progression. Nat Med. 3:338-40.

Philpott SM. (2003) HIV-1 coreceptor usage, transmission, and disease progression. Curr HIV Res. 2:217-27.

Proctor NJ, Tucker GT, Rostami-Hodjegan A.(2004) Predicting drug clearance from recombinantly expressed CYPs: intersystem extrapolation factors. Xenobiotica. 34:151-78.

Roy JN, Lajoie J, Zijenah LS, Barama A, Poirier C, Ward BJ, Roger M. (2005) CYP3A5 genetic polymorphisms in different ethnic populations. Drug Metab Dispos. 33: 884-7.

Tseng E, Walsky RL, Luzietti RA, Jr, Harris JJ, Kosa RE, Goosen TC, Zientek MA, Obach RS. (2014) Relative contributions of cytochrome CYP3A4 versus CYP3A5 for CYP3A-cleared drugs

assessed in vitro using a CYP3A4-selective inactivator (CYP3cide). Drug Metab Dispos 42:1163–1173.

Vourvahis M, Fang J, Checchio T, Milton A, Weatherley B, McFadyen L, Heera J. (2013) Pharmacokinetics, safety, and tolerability of maraviroc in HIV-negative subjects with impaired renal function. HIV Clin Trials. 14: 99-109.

Vourvahis M, McFadyen L, Heera J, and Clark A (2015) Clinical Relevance of CYP3A5 Genotype on Maraviroc Exposures. Drug Metab Dispos 43: 771-772;

Walsky RL, Obach RS, Hyland R, Kang P, Zhou S, West M, Geoghegan KF, Helal CJ, Walker GS, Goosen TC, and Zientek MA (2012) Selective Mechanism-Based Inactivation of CYP3A4 by CYP3cide (PF-04981517) and Its Utility as an In Vitro Tool for Delineating the Relative Roles of CYP3A4 versus CYP3A5 in the Metabolism of Drugs. Drug Metab. Dispos. 40: 1686-1697.

DMD Fast Forward. Published on February 23, 2018 as DOI: 10.1124/dmd.117.079855
This article has not been copyedited and formatted. The final version may differ from this version.

Legends for Figures

Figure 1. HPLC-MS Chromatograms of Metabolites Generated in Incubations of MVC with Cytochrome P450 3A4 and 3A5. The chromatograms are extracted ion traces for *m/z* 530.3278 (5 ppm width). The peaks are annotated with the notation for 2- and 3-OH-MVC and hydroxymethylMVC. Top panel: CYP3A4. Bottom panel: CYP3A5.

Figure 2. Abbreviated ^{1}H NMR spectra of A) MVC (bottom), fraction 1: (1S,2S)-2-OH-MVC (middle), and fraction 4: (1R,2R)-2-OH-MVC (top); B) MVC (bottom), fraction 2: (1S,3R)-3-OH-MVC (middle), and fraction 3: (1S,3S)-3-OH-MVC (top).

Figure 3. Abbreviated ^{1}H NMR spectrum of hydroxymethylMVC and MVC.

Figure 4. Metabolism of 2- and 3-OH-MVC Diastereomers by Cytochrome P450 3A4 to 2,3-DiOH-MVC.

Figure 5. Substrate saturation curves of (1S,2S), (1R,2R), (1S,3S), (1S,3R), and hydroxymethylMVC formation in pooled human liver microsomes, pooled CYP3A5 *1/*1 human liver microsomes, pooled CYP3A5 *3/*3 liver microsomes, and recombinant human CYP3A4 and CYP3A5. Plots on the left are in human liver microsomes and plots on the right are in recombinant systems.

Figure 6. Formation of (1S,2S)-2-OH-MVC, (1R,2R)-2-OH-MVC, (1S,3S)-3-OH-MVC, (1S,3R)-3-OH-MVC, and hydroxymethylMVC in pooled human liver microsomes, pooled CYP3A5 *1/*1 human liver microsomes, pooled CYP3A5 *3/*3 liver microsomes in the presence and absence of selective CYP3A and CYP3A4 inhibitors, ketoconazole and CYP3cide, respectively. Percent values represent the calculated contribution by CYP3A5.

Figure 7. Activity Correlation of (1S,2S)-2-OH-MVC formation to T5 N-oxide formation in pooled and individual CYP3A5 *1/*1, CYP3A5 *1/*3, and CYP3A5 *3/*3 liver microsomes. HLM102 represents a 50-donor HLM pool. The dotted lines of regression represent the 90% prediction bands. The Pearson r correlation value was 0.810 ($p<0.0001$).

Figure 8. Metabolism Scheme of MVC by CYP3A4 and CYP3A5. The percentages denote the estimated CYP3A5 contribution to each metabolite in CYP3A5 *1/*1 HLM.

Table 1. Enzyme kinetic parameters for maraviroc metabolic pathways in pooled HLM from CYP3A5*1/*1 and CYP3A5*3/*3 donors and recombinant human CYP 3A4 and CYP 3A5.

	Kinetic Parameters[a]	(1S,2S)-2-OH-MVC	(1S,3R)-3-OH-MVC	(1S,3S)-3-OH-MVC	(1R,2R)-2-OH-MVC	Hydroxymethyl MVC	Total
rhCYP3A4	K_M ± SE	10.4 ± 0.476	10.1 ± 0.504	10.0 ± 0.524	10.5 ± 0.556	10.9 ± 0.452	
	Vmax ± SE	0.96 ± 0.0117	1.31 ± 0.0173	0.81 ± 0.0112	0.57 ± 0.00808	3.41 ± 0.0380	
	$CL_{int,app}$	0.09	0.13	0.08	0.05	0.31	0.67
rhCYP3A5	K_M ± SE	8.4 ± 0.622	7.8 ± 0.439	7.6 ± 0.417	8.0 ± 0.466	8.2 ± 0.458	
	Vmax ± SE	7.3 ± 0.139	0.8 ± 0.0116	0.5 ± 0.00687	0.8 ± 0.0115	1.4 ± 0.0192	
	$CL_{int,app}$	0.87	0.11	0.07	0.10	0.16	1.31
HLM-102	K_M ± SE	12.9 ± 0.477	13.3 ± 0.534	12.5 ± 0.584	13.4 ± 0.517	15.5 ± 0.707	
	Vmax ± SE	121 ± 1.26	113 ± 1.27	89.3 ± 1.16	75.7 ± 0.824	216 ± 2.87	
	$CL_{int,app}$	9.4	8.5	7.1	5.7	14.0	44.6
	$CL_{int,app,sc}$	8.9	8.0	6.7	5.3	13.2	42.2
HLM CYP3A5 *1/*1	K_M ± SE	15.6 ± 0.778	17.4 ± 1.02	16.9±0.927	18.0±1.07	18.6±1.00	
	Vmax ± SE	245 ± 3.56	65.6±1.15	54.3±0.884	52.5±0.945	119±1.95	
	$CL_{int,app}$	15.6	3.8	3.2	2.9	6.4	32.0
	$CL_{int,app,sc}$	14.8	3.6	3.0	2.8	6.1	30.2
HLM CYP3A5 *3/*3	K_M ± SE	15.5±0.779	15.9±0.589	15.9±0.714	17.1±0.807	17.0±0.696	
	Vmax ± SE	81.3±1.19	98.7±1.07	80.2±1.06	66.8±0.941	182±2.22	
	$CL_{int,app}$	5.2	6.2	5.0	3.9	10.7	31.1
	$CL_{int,app,sc}$	5.0	5.9	4.8	3.7	10.1	29.4

[a]Units - $CLint_{,app}$: µL/min/pmol or µL/min/mg; $K_{M:}$ µM ; V_{max}: pmol/min/pmol P450 or pmol/min/mg protein
Mean data from three replicates

DMD Fast Forward. Published on February 23, 2018 as DOI: 10.1124/dmd.117.079855
This article has not been copyedited and formatted. The final version may differ from this version.

Table 2. Estimation of CYP3A5 fraction metabolized in human liver microsomes pooled from CYP3A5 extensive metabolizers

	HLM CYP3A5*1/*1 $Cl_{int,app}$ (μL/min/mg)	f_{CL}	Fraction of CYP3A5 Contribution Estimated by Differential Inhibition by CYP3cide and Ketoconazole	Estimated f_m for CYP3A5
(1S,2S)-2-OH-MVC	15.6	0.5	0.42	0.21
(1S,3R)-3-OH-MVC	3.8	0.1	0.08	0.01
(1S,3S)-3-OH-MVC	3.2	0.1	0.09	0.01
(1R,2R)-2-OH-MVC	2.9	0.1	0.14	0.01
HydroxymethylMVC	6.4	0.2	0.06	0.01
$CL_{int,app,all}$ Total	31.9			0.25

f_{CL}: fraction of total metabolic clearance
f_m: fraction metabolized

Figure 1

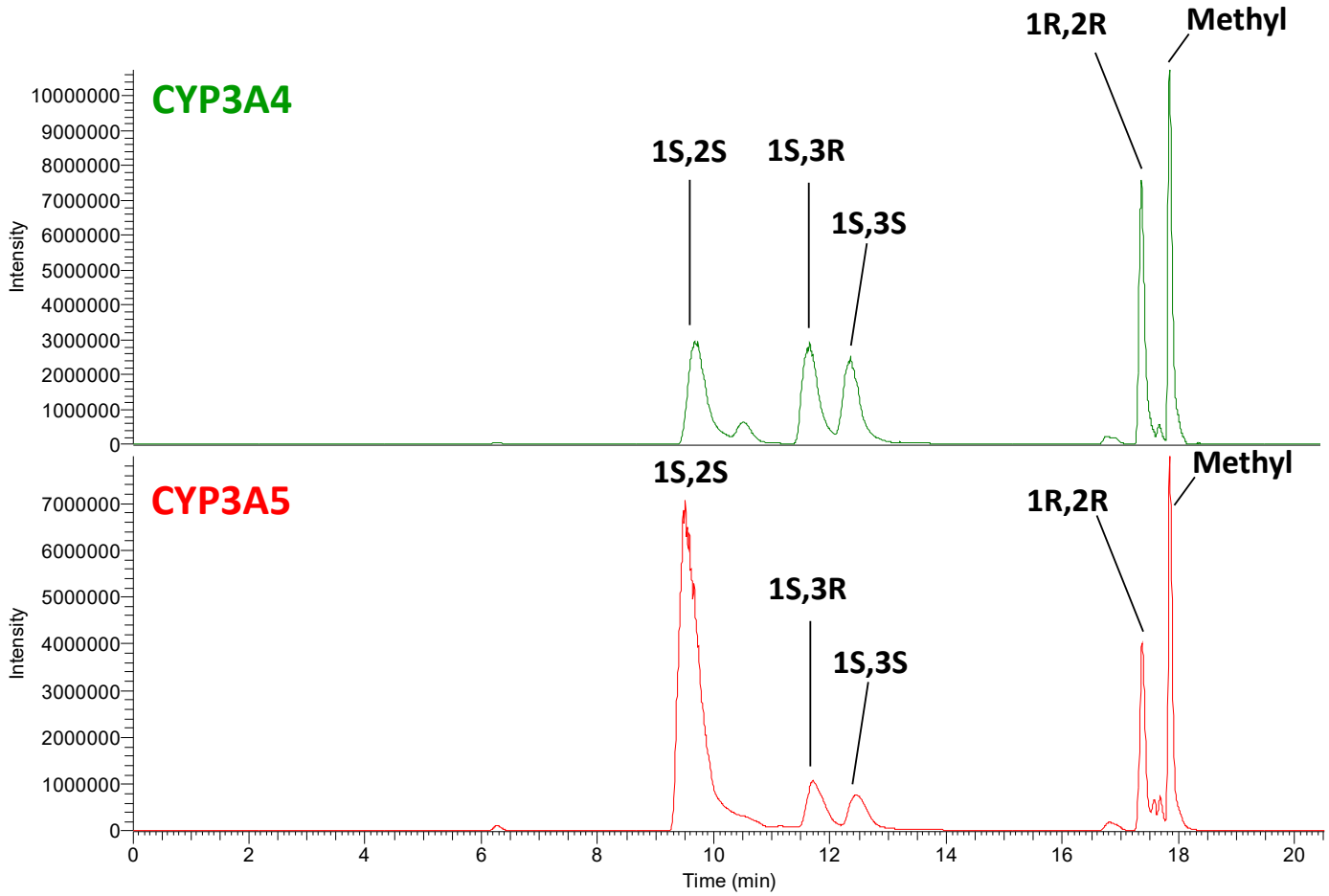

Figure 2

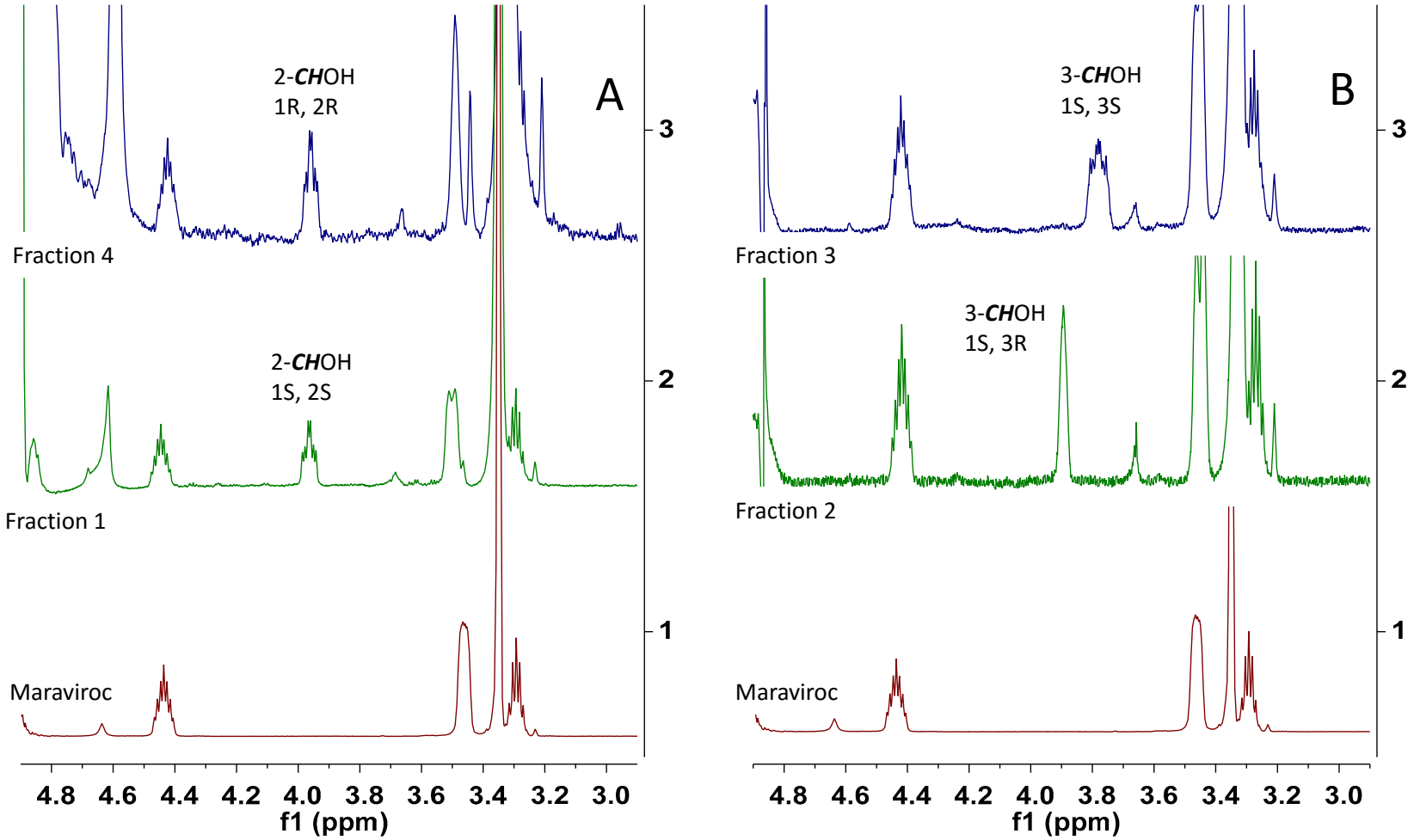

Figure 3

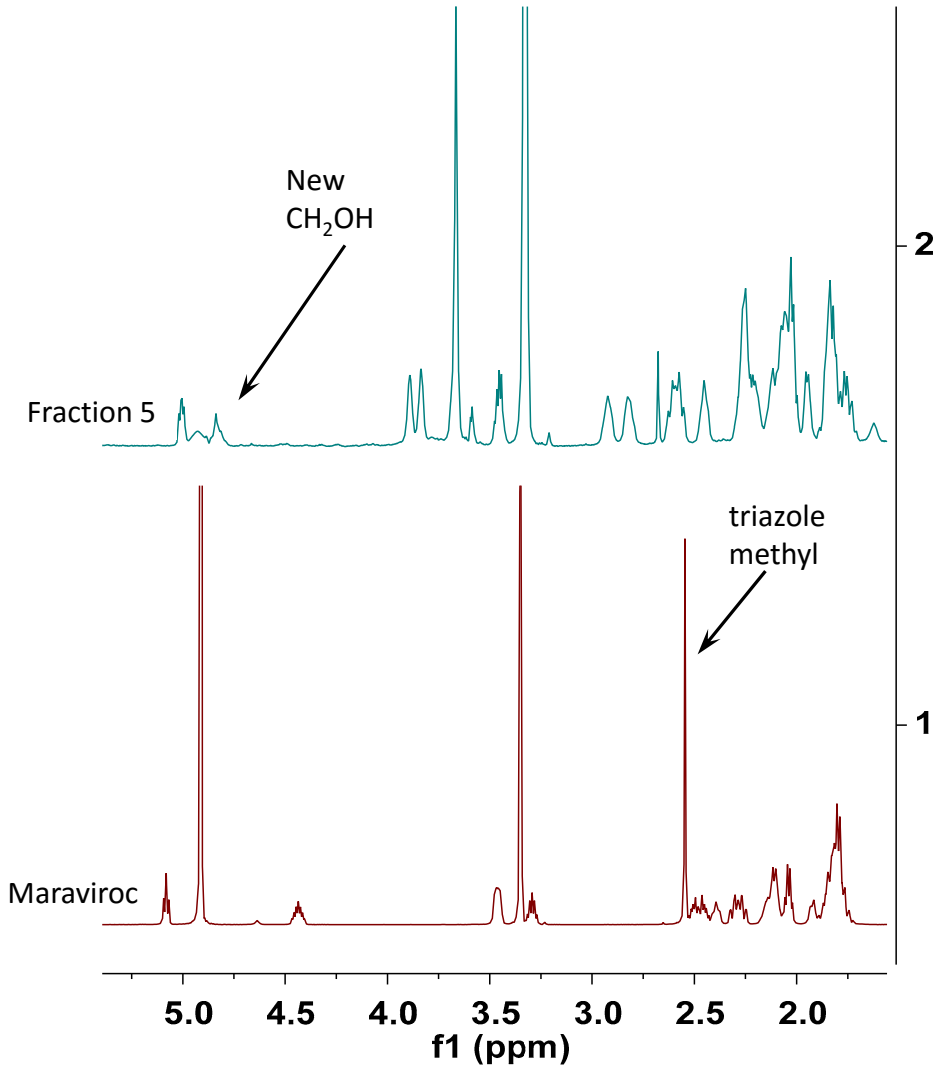

Figure 4

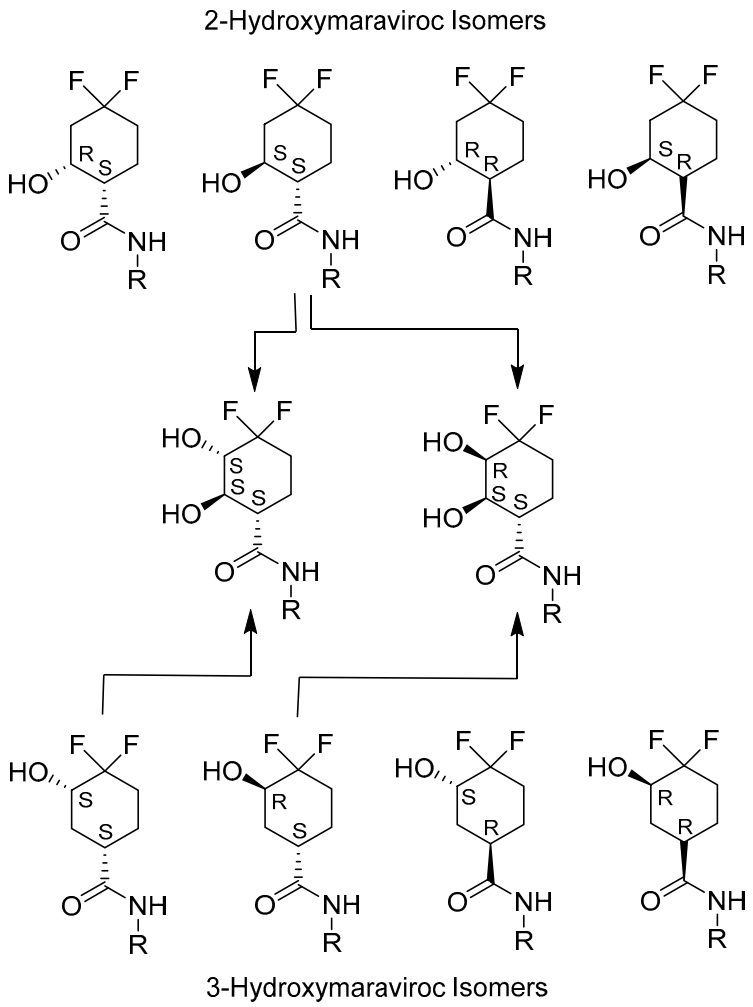

DMD Fast Forward. Published on February 23, 2018 as DOI: 10.1124/dmd.117.079855
This article has not been copyedited and formatted. The final version may differ from this version.

Figure 5

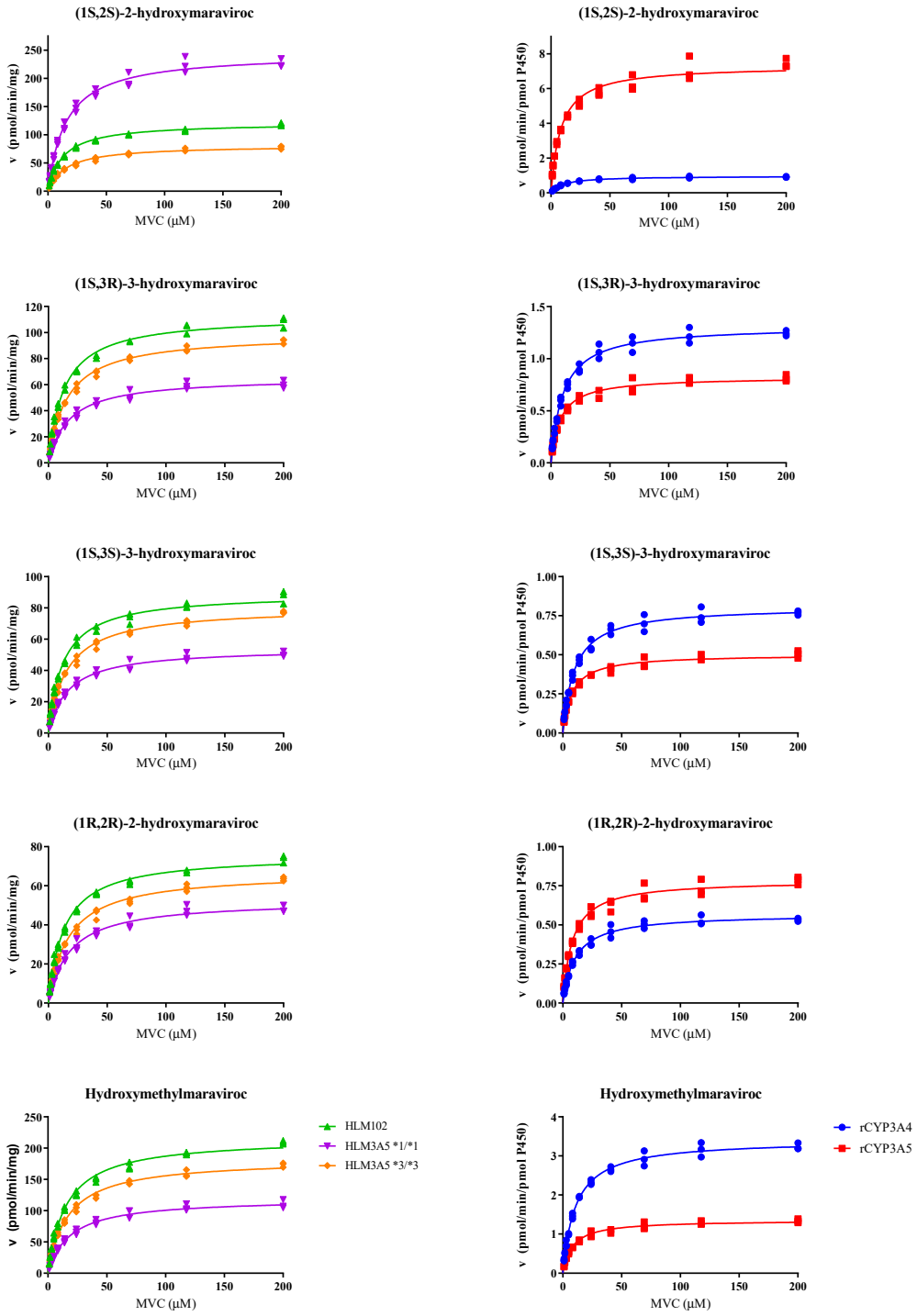

Figure 6

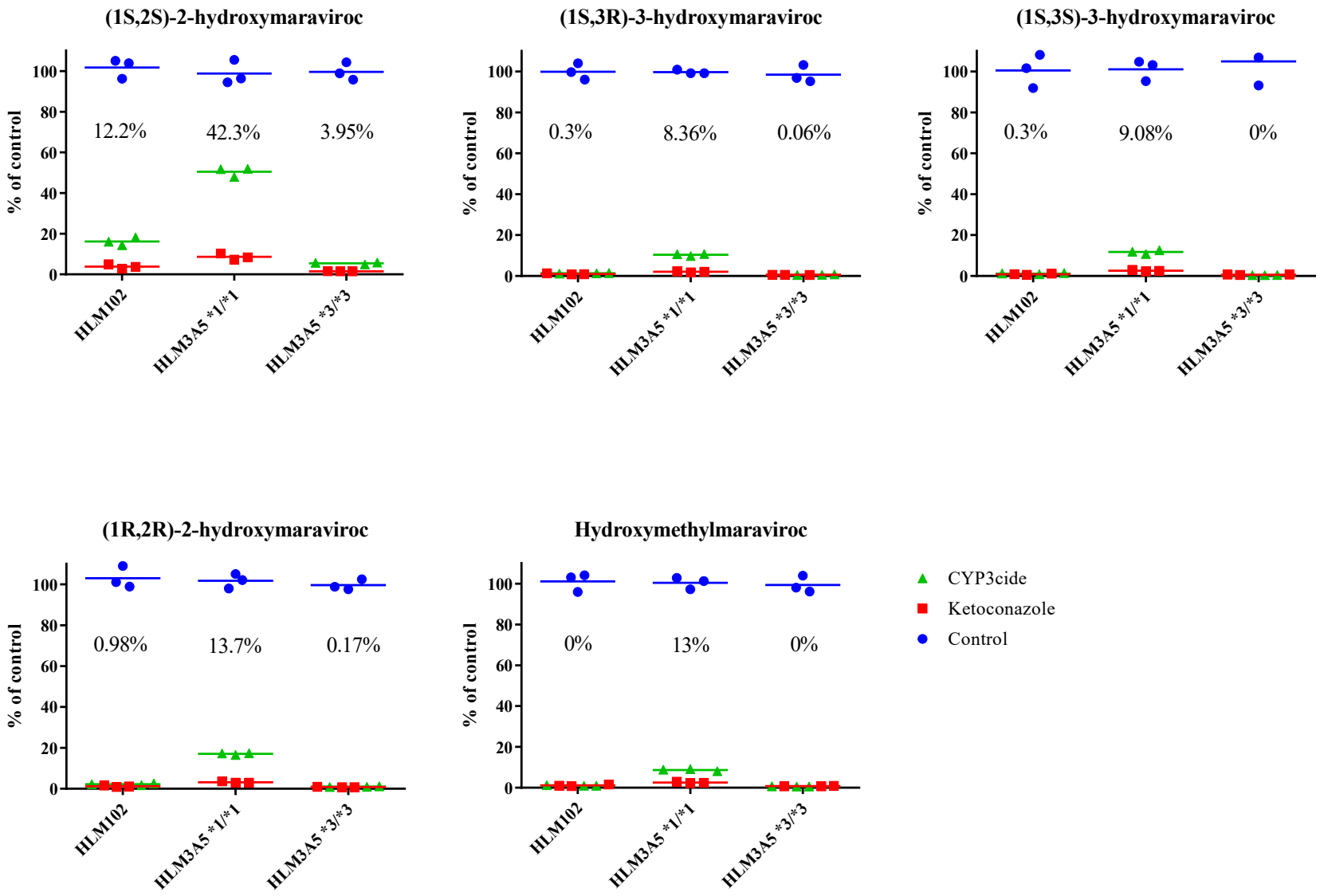

Figure 7

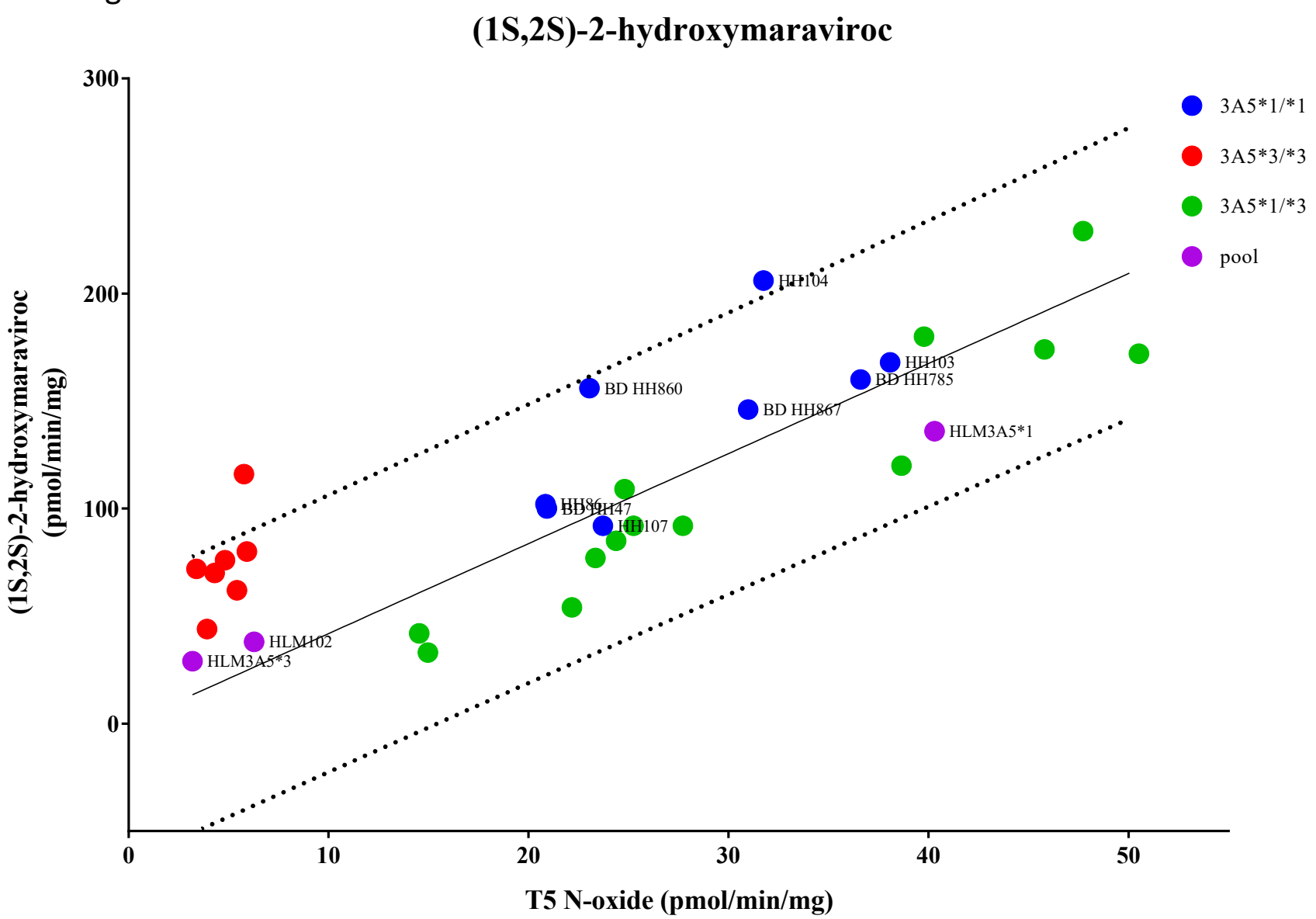

Figure 8